THE JOURNAL OF PHYSICAL CHEMISTRY A

Article

Cite This: J. Phys. Chem. A 2019, 123, 10919−10929

pubs.acs.org/JPCA

Structural and Electronic Rearrangements in Fe_2S_2, Fe_3S_4, and Fe_4S_4 Atomic Clusters under the Attack of NO, CO, and O_2

Fadila Amitouche,*[,†] Farida Saad,[†] Slimane Tazibt,[‡] Said Bouarab,[†] and Andrés Vega[§]

[†]Laboratoire de Physique et Chimie Quantique, Faculté des Sciences and [‡]Faculté du Génie Electrique et d'Informatique, Université Mouloud Mammeri de Tizi-Ouzou, B.P. No. 17 RP, 15000 Tizi-Ouzou, Algeria

[§]Departamento de Física Teórica, Atómica y Óptica, Universidad de Valladolid, Paseo Belèn 7, E-47011 Valladolid, Spain

ABSTRACT: We report results, based on density functional theory−generalized gradient approximation calculations, that shed light on how NO, CO, and O_2 interact with Fe_2S_2, Fe_3S_4, and Fe_4S_4 clusters and how they modify their structural and electronic properties. The interest in these small iron sulfide clusters comes from the fact that they are at the protein cores and that elucidating fundamental aspects of their interaction with those light molecules which are known to modify their functionality may help in understanding complex behaviors in biological systems. CO and NO are found to bind molecularly, leading to moderate relaxations in the clusters, but nevertheless to changes in the spin-polarized electronic structure and related properties. In contrast, dissociative chemisorption of O_2 is much more stable than molecular adsorption, giving rise to significant structural distortions, particularly in Fe_4S_4 that splits into two Fe_2S_2 subclusters. As a consequence, oxygen tends to strongly reduce the spin polarization in Fe and to weaken the Fe−Fe interaction inducing antiparallel couplings that, in the case of Fe_4S_4, clearly arise from indirect Fe−Fe exchange coupling mediated by O. The three molecules (particularly CO) enhance the stability of the iron−sulfur clusters. This increase is noticeably more pronounced for Fe_2S_2 than for the other iron−sulfur clusters of different compositions, a result that correlates with the fact that in recent experiments of CO reaction with Fe_mS_m (m = 1−4), the Fe_2S_2CO product results as a prominent one.

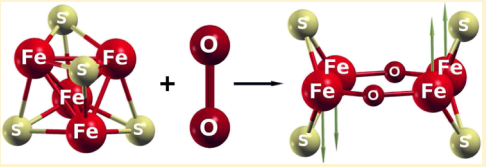

INTRODUCTION

Iron−sulfur proteins are an ancient and important class of proteins that constitute a hot topic in several research fields and that are still full of surprises.[1] They were discovered in the 60s in the context of studies on photosynthetic, nitrogen-fixing bacteria and submitochondrial parts of mammalian cells.[2] They have since been found in all living organisms, including archaea and bacteria. Research in this field is very active, revealing unexpected functions, structures, and redox states.[3] Fe−S proteins are characterized by the presence of inorganic clusters of iron and sulfide with one to eight ferric (Fe^{3+}) or ferrous (Fe^{2+}) ions and about the same number of sulfides (S^{2-}). Despite their extraordinary versatility, the composition of Fe−S metal sites is relatively simple; the iron coordination is tetrahedral throughout. The basic structural principle of iron sulfide clusters is the rhombic Fe_2S_2, which can be combined in multiple ways to lead to canonical [2Fe−2S], [3Fe−4S], and [4Fe−4S] clusters and more complex structures. Because they can access various redox states, these clusters are ideal for electron-transfer and redox reactions. In biological electron transport chains, these [Fe−S] clusters have versatile electrochemical properties with reduction potentials ranging from more than 500 mV to less than −500 mV. In addition to their electron-transfer function, Fe−S clusters act as catalytic centers and sensors of iron and oxygen.[2] Furthermore, these clusters were found to be sensitive to molecular oxygen and oxidants, such as hydrogen peroxide (H_2O_2), nitric oxide (NO), and carbon monoxide (CO), which can be of functional significance. Among the light diatomic molecules, NO is one of the most versatile reactants; it may react as NO^0 and NO^+ or even as NO^- and has no diffusion barrier or very low. NO also has a high affinity to iron and easily displaces or breaks the sulfur ligands to the iron skeleton. Structural, electronic, and magnetic properties of Fe-based systems can dramatically change under oxidation. Besides, the interaction between iron and oxygen in these clusters is relevant to understand important chemical and biochemical processes, such as corrosion and oxygen transport in biological systems.

To understand the intrinsic electronic properties of Fe−S active centers, the most common iron sulfide Fe_2S_2, Fe_3S_4, and Fe_4S_4 clusters contained in proteins have been widely investigated in the gas phase from the experimental side. Fe−S cluster anions ($Fe_nS_m^-$, n = 1−6, m = 1−6) have been characterized using photoelectron spectroscopy (PES) through which the electron affinities (EAs) and the vertical detachment energies (VDEs) were determined.[4] The most stable anions were found to be those with $n = m$ or $n = m \pm 1$, demonstrating that $Fe_nS_m^-$ species ($n = m$ = 2, 3, 4, 6), which are iron−sulfur centers in proteins, are also stable in the gas phase. PES data and inferred geometric properties of iron sulfide anionic clusters ($Fe_nS_m^-$, n = 1−8, m = 2−6) have also been reported in the literature together with chemical probe

Received: August 28, 2019
Revised: November 28, 2019
Published: December 3, 2019

DOI: 10.1021/acs.jpca.9b08201
J. Phys. Chem. A 2019, 123, 10919−10929

measurements for the corresponding cations.[5] A noticeable change of EAs of $Fe_nS_m^-$ clusters at the equiatomic composition ($n = m$) was observed. Their reactivity to NH_3 and C_2H_2 is enhanced around $n = m$. Those results suggest that the cluster structures seem to be formed by alternating bonds (−S−Fe−S−Fe−) between Fe and S atoms, resembling those of an active site in iron sulfide proteins.[1] Species could be considered to have structures with $Fe_nS_m^+$ cores surrounded by some peripheral S atoms. Experimental studies on neutral iron sulfide Fe_mS_n ($m = 1-6$, $n = 1-6$) clusters generated by laser ablation[6] showed that the most intense mass peaks correspond to FeS, Fe_2S_2, Fe_3S_3, and Fe_4S_4. The relatively high Fe_mS_n signal intensities were found at $n = m$ for $m = 1-4$. The reaction of these clusters with CO was also studied. It was found that with FeS the reaction leads to the formation of the carbonyl sulfide, with Fe_2S_2, it produces Fe_2S_2−CO, and with Fe_3S_3 and Fe_4S_4, no products were detected. More recently, a PES study of sulfur cluster anions $(FeS)_m^-$ ($m = 2-8$) where VDEs and EAs were measured suggests the possible coexistence of multiple spin states of these clusters.[7]

From the theoretical point of view, most calculations on Fe_2S_2, Fe_3S_4, and Fe_4S_4 clusters have been performed either in protein-simulated environments[8−15] or free of any ligands.[7,16−20] In a previous study, based on density functional theory (DFT),[18] our group found that those freestanding clusters conserve the geometries they have inside core proteins, apart from small distortions.[18] Compared to experimental data in proteins, the bond length of a geometry-optimized structure for the Fe_3S_4 cluster is compressed within ∼2−5%. The aim of the present work is to carry out a systematical theoretical study of the structural, electronic, and magnetic properties of Fe_2S_2, Fe_3S_4, and Fe_4S_4 clusters attacked by NO, CO, and O_2 molecules, which are known to alter the functions of proteins. The iron−sulfur proteins in which the iron atoms are not fully coordinated by sulfur are particularly vulnerable to the attack of NO.[21−25] The ability of carbon monoxide (CO) to bind to heme proteins and to alter their function and/or metabolism is well known. The iron−sulfur clusters are generally known to be oxygen-sensitive. However, the mechanism of the oxidation of these systems is very complex because there exist sharp differences in oxygen tolerance of the different FeS clusters.[26−35] In this context, an analysis, by means of DFT, of differences in oxygen sensitivity of Fe_2S_2, Fe_3S_4, and Fe_4S_4 clusters coordinated by cysteine residues was carried out by Bruska et al.[31] It was found that significant structural distortions are required to bind O_2 exothermically to $[Fe_2S_2]$ and $[Fe_3S_4]$, while small conformational changes allow for the thermodynamically favorable coordination of molecular oxygen to $[Fe_4S_4]$ and $[Fe_4S_3]$ clusters. Another theoretical work was performed by the same authors[32] on the decomposition of Fe−S clusters in [FeFe] hydrogenase upon O_2 attack. The degradation pathways of the $[Fe_4S_4]$ cubane, proposed and compared to the decomposition of $[Fe_4S_4]$ in other enzymes,[33−35] are accompanied by significant structural distortions. In view of the information presented above, we found it appealing to study how these three molecules interact with the freestanding Fe_2S_2, Fe_3S_4, and Fe_4S_4 clusters and how they change their structural, magnetic, and electronic indicators among which the VDEs and EAs have been measured.

After a description of our theoretical approach in the next section, we analyze the lowest-energy structures of Fe_2S_2, Fe_3S_4, and Fe_4S_4 clusters in comparison with available theoretical and experimental results. Then, we present the results for NO, CO, and O_2 interactions with these host clusters. The last part of the discussion is devoted to analyze the main effects of such interactions on the stability, structure, magnetic properties, and electronic indicators of the Fe−S clusters. The main conclusions are summarized at the end.

■ COMPUTATIONAL METHOD

The calculations have been performed using DFT as implemented in the Vienna ab initio simulation package (VASP),[36] which solves the spin-polarized Kohn−Sham equations in an augmented plane-wave basis set by using the projector augmented wave (PAW) method[37,38] to treat the core interactions. The PAW approach produces the exact all-electron potentials and charge densities without the need of including nonlinear core corrections, which are particularly important for magnetic systems. Thus, it can be considered as an efficient quasi-all-electron approach. The basis set contains plane waves with a maximum kinetic energy of 400 eV. The exchange and the correlation effects were treated in the generalized gradient approximation by using the Perdew−Burke−Ernzerhof (PBE) functional.[39]

We note that many authors[16−19] agree on the lowest-energy structures of Fe_2S_2, Fe_3S_4, and Fe_4S_4 clusters, apart from small distortions. As reported above, by using the SIESTA code[40,41] that employs Troullier−Martins pseudopotentials instead of PAWs for the core interactions and numerical pseudoatomic orbitals instead of plane waves as basis sets, our group found that these clusters conserve essentially the geometries they have inside core proteins.[18] To have the references of the host clusters, we reoptimized those structures with VASP. For seeking the low-lying structures of [Fe−S]−NO, −CO, $-O_2$, we considered many initial configurations: (1) by adsorbing molecularly NO, CO, and O_2 oxidants on all possible sites of bare Fe_2S_2, Fe_3S_4, and Fe_4S_4 isomers (first, second, and sometimes third isomers) calculated beforehand and by considering all the possible chemical bonds such as −Fe(S)−NO, −Fe(S)−CO, −Fe(S)−O_2, −Fe(S)−ON, −Fe(S)−OC··· and (2) by adsorbing (or placing) the two atoms of the molecules (dissociated) on different sites (or on different substitutional sites).

The cubic supercell throughout the calculations is chosen with an edge of 15 Å, being large enough to suppress any interaction between the periodically repeated images of the clusters. The integration over the Brillouin zone is done at the Γ point only. In the structural optimization process, we relaxed the atoms until the forces dropped below a threshold value of 0.001 eV/Å. We included dipole and quadrupole corrections in the calculations, which can be especially important for the charged species. Geometric, electronic, and magnetic degrees of freedom were relaxed until the change in total energy between successive iteration steps reached 10^{-7} eV.

The relative stability of different spin isomers was also checked by performing calculations for different magnetic states to be sure of the total spin of the putative ground state. We explicitly considered possible noncollinear arrangements by exploring an important number of spin configurations, especially in Fe_3S_4 and Fe_3S_4−CO, −NO, and $-O_2$ clusters having an odd number of iron atoms. All of them converged to collinear states. We note that VASP evaluates the local spin moments and charges by projecting the plane-wave components of the eigenstates onto spherical waves inside slightly overlapping atomic spheres. Although this gives a qualitative

DOI: 10.1021/acs.jpca.9b08201
J. Phys. Chem. A 2019, 123, 10919−10929

Table 1. Calculated Values[a] for $FeS^{0/\pm}$ Dimers Compared to Experimental Data

dimer		MM (μ_B)	r (Å)	ω (cm^{-1})	VDE (eV)	AEA (eV)	IP (eV)
FeS	PBE	4	2.00	537			8.00
	B3LYP	4	2.03	415			8.17
	exptl works		2.04[b]	540[c]			8.3 ± 0.3[d]
			520 ± 30[e]				
FeS^-	PBE	3	2.04	460	1.72	1.69	
	B3LYP	3	2.07	458	1.73	1.70	
	exptl works		2.18[e]	450[e]	1.85 ± 0.10[f]	1.72 ± 0.10[f]	
					2.04 ± 0.09[g,h]	1.76 ± 0.10[g,h]	
FeS^+	PBE	5	2.01	478			
	B3LYP	5	2.03	421			
	exptl works		2.05[d]	448[d]			

[a]Magnetic moment MM, bond length r, vibrational frequency ω, vertical detachment energy VDE, adiabatic electronic affinity AEA, and ionization potential IP. [b]Reference 49. [c]Reference 50. [d]Reference 51. [e]Reference 52. [f]Reference 53. [g]Reference 4. [h]Reference 54.

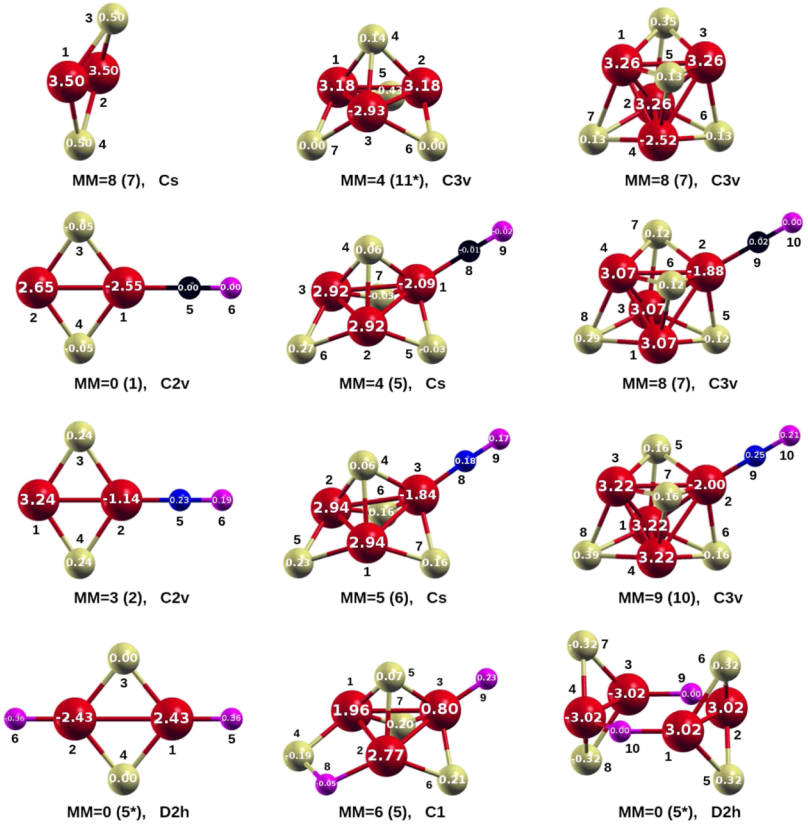

Figure 1. Putative ground-state structures of isolated Fe_2S_2, Fe_3S_4, and Fe_4S_4 (first line) and their corresponding ones upon CO (second line), NO (third line), and O_2 (fourth line) adsorption, with their point-group symmetry and total magnetic moment MM (in units of μ_B). The corresponding total moment of the anionic state is given in parenthesis when the geometrical structure is preserved. For anionic states having magnetic moment that differ in more than ± 1 μ_B with respect to the neutral state, that moment is highlighted by * and those cases are explicitly discussed in the text. The local spin moments are given in units of μ_B inside the atomic spheres, while the bond lengths are given in Table 2 according to the labels of the different atoms. Fe (red), S (yellow), O (magenta), C (black), and N (blue) spheres represent the different atoms of the clusters.

picture of the local distribution of such magnitudes, this projection depends on the choice of the atomic radius, and the sum of the local quantities is not, in general, identical to the total value. Therefore, we performed an alternative analysis by using Bader's method,[42−44] which is based on partitioning the cluster into atomic volumes by locating the zero-flux surfaces of the electron density field.

To confirm that the optimized geometries correspond to a local minimum in potential energy, an analysis of harmonic vibration frequencies was performed. In the case of an imaginary frequency, we carried out a new relaxation along the corresponding unstable normal coordinate with more stringent convergence criteria. In most of the calculated clusters, the optimized geometries of the neutral and anionic states are very similar (apart from small distortions). Then, we report the geometries of the neutral species and explicitly mention, along the discussion, those cases where differences arise.

Benchmark calculations of bond length, vibrational frequency, VDE, adiabatic electron affinity (AEA), and ionization potential (IP) of $Fe_2^{0/\pm}$, $S_2^{0/\pm}$ and $FeS^{0/\pm}$ dimers showed a fairly good agreement between the calculated and the

DOI: 10.1021/acs.jpca.9b08201
J. Phys. Chem. A 2019, 123, 10919−10929

Table 2. Interatomic Distances r_{ij} (Å) in Fe_2S_2, Fe_3S_4, and Fe_4S_4 Clusters and in Their Corresponding Ones upon CO, NO, and O_2 Adsorption According to the Labels of the Different Atoms of Figure 1

Fe_2S_2	Fe_3S_4	Fe_4S_4
$r_{13} = r_{23} = r_{14} = r_{24} = 2.20$	$r_{12} = r_{23} = r_{31} = 2.38$	$r_{12} = r_{13} = r_{23} = 2.61$
$r_{12} = 2.21$	$r_{41} = r_{42} = r_{43} = 2.26$	$r_{14} = r_{24} = r_{34} = 2.38$
	$r_{17} = r_{25} = r_{73} = r_{36} = r_{62} = r_{51} = 2.18$	$r_{16} = r_{18} = r_{26} = r_{27} = r_{37} = r_{38} = 2.28$
	$r_{15} = r_{25} = r_{35} = 2.26$	
	$r_{46} = r_{47} = r_{48} = 2.37$	
Fe_2S_2–CO	Fe_3S_4–CO	Fe_4S_4–CO
$r_{12} = 2.43$	$r_{12} = r_{13} = 2.53$	$r_{14} = r_{24} = r_{34} = 2.59$
$r_{23} = r_{24} = 2.10$	$r_{15} = r_{17} = 2.16$	$r_{12} = r_{23} = r_{34} = 2.40$
$r_{13} = r_{14} = 2.14$	$r_{14} = 2.18$, $r_{18} = 1.84$	$r_{15} = r_{25} = r_{35} = 2.29$
$r_{15} = 1.83$	$r_{25} = r_{37} = 2.13$	$r_{16} = r_{18} = r_{26} = r_{27} = r_{37} = r_{38} = 2.26$
$r_{56} = 1.16$	$r_{24} = r_{34} = 2.26$	$r_{46} = r_{47} = r_{48} = 2.22$
	$r_{26} = r_{36} = 2.19$	$r_{49} = 1.80$, $r_{910} = 1.16$
	$r_{23} = 2.39$, $r_{89} = 1.16$	
Fe_2S_2–NO	Fe_3S_4–NO	Fe_4S_4–NO
$r_{13} = r_{14} = 2.16$	$r_{12} = r_{13} = 2.56$	$r_{14} = r_{24} = r_{34} = 2.63$
$r_{23} = r_{24} = 2.12$	$r_{14} = 2.22$, $r_{23} = 2.41$	$r_{12} = r_{13} = r_{23} = 2.41$
$r_{12} = 2.40$	$r_{15} = r_{17} = 2.21$	$r_{15} = r_{25} = r_{35} = 2.31$
$r_{15} = 1.68$	$r_{25} = r_{37} = 2.13$	$r_{16} = r_{18} = r_{26} = r_{27} = r_{37} = r_{38} = 2.27$
$r_{56} = 1.19$	$r_{26} = r_{36} = 2.19$	$r_{46} = r_{47} = r_{48} = 2.27$
	$r_{24} = r_{34} = 2.24$	$r_{49} = 1.66$, $r_{910} = 1.18$
	$r_{18} = 1.67$, $r_{89} = 1.18$	
Fe_2S_2–O_2	Fe_3S_4–O_2	Fe_4S_4–O_2
$r_{13} = r_{14} = r_{23} = r_{24} = 2.11$	$r_{13} = r_{23} = 2.51$	$r_{13} = r_{24} = 2.42$
$r_{15} = r_{26} = 1.62$	$r_{12} = 2.39$, $r_{14} = 2.10$	$r_{19} = r_{29} = r_{310} = r_{410} = 1.75$
$r_{12} = 2.65$	$r_{15} = 2.16$, $r_{17} = 2.01$	$r_{15} = r_{18} = r_{26}r_{27} = r_{35} = r_{38} = r_{46} = r_{47} = 2.17$
	$r_{25} = 2.23$, $r_{26} = 2.12$	
	$r_{28} = 1.88$, $r_{35} = 2.19$	
	$r_{36} = 2.14$, $r_{37} = 2.15$	
	$r_{39} = 1.59$, $r_{48} = 1.61$	

measured values.[45] Besides, the calculated bond lengths for CO (1.14 Å), NO (1.17 Å), and O_2 (1.22 Å) are also in very good agreement with their respective experimental values[46] 1.13, 1.15, and 1.21 Å. Another relevant aspect is the treatment of exact exchange and the concomitant self-interaction correction for a right description of the structural and electronic properties and spin states. This problem was addressed by some authors such as Reiher et al.[47] and Paulsen et al.[48] For example, it was shown by Reiher et al.[47] that the energy splitting depends linearly on the coefficient of the exact exchange admixture; the B3LYP functional with 15% exact exchange provides a good description of the energetics of some Fe(II)–S complexes. As a further benchmark, we performed additional calculations for the $FeS^{0/\pm}$ dimers using the B3LYP functional with 15% exact exchange. In Table 1, we compare relevant structural and electronic magnitudes obtained with PBE with those obtained with the B3LYP functional and also with data from available experiments. The spin state is the same in both approaches, independently of the charge state, resulting in a spin moment 1 μ_B lower (higher) in the anionic (cationic) cluster than in the neutral one. Concerning the structural properties, both theoretical approaches slightly underestimate the experimental value of the interatomic distance (by about 1% more with the PBE functional). The vibrational frequency of the charged clusters is obtained within the same degree of accuracy within both theoretical approaches as compared with the experiment, but for the neutral cluster the value obtained with B3LYP departs from the experimental value by about 20% while only by 6% in the PBE approach. With regard to the electronic indicators, both theoretical approaches give consistent values (slightly underestimated) for the AEA, VDE, and IP as compared with the experimental data. The largest difference between PBE and B3LYP concerns the IP, which is about 2% lower with PBE than with B3LYP.

RESULTS AND DISCUSSION

Structural and Magnetic Properties. *Fe_2S_2, Fe_3S_4, and Fe_4S_4 Clusters.* We report in Figure 1 the most stable atomic arrangements of Fe_2S_2, Fe_3S_4, and Fe_4S_4 with their point-group symmetry and their spin states. The bond lengths are given in Table 2 according to the labels of the different atoms. These are in agreement with previous calculations.[16−19] The low-lying isomers can be obtained from the authors upon request.

The ground state of Fe_2S_2 has a similar structure as the one present at some cores of proteins, with alternating Fe and S atoms.[55−58] It consists of a 3D buckled rhombus of C_s symmetry in which the Fe_2S entities form a dihedral angle of 155.9° (Figure 1). In this configuration, the Fe–Fe magnetic coupling is parallel, and the resulting total moment is 8 μ_B contributed by both Fe and S atoms with 3.50 and 0.50 μ_B, respectively. The planar rhombic structure associated with a spin-polarized electronic density distribution with antiparallel couplings in the singlet state is the first isomer at just 0.01 eV from the ground state. Compared to the ground state, its Fe–Fe bond is enlarged by about 10%, whereas the Fe–S bond is decreased by 3%, and no structural distortion takes place.

DOI: 10.1021/acs.jpca.9b08201
J. Phys. Chem. A 2019, 123, 10919−10929

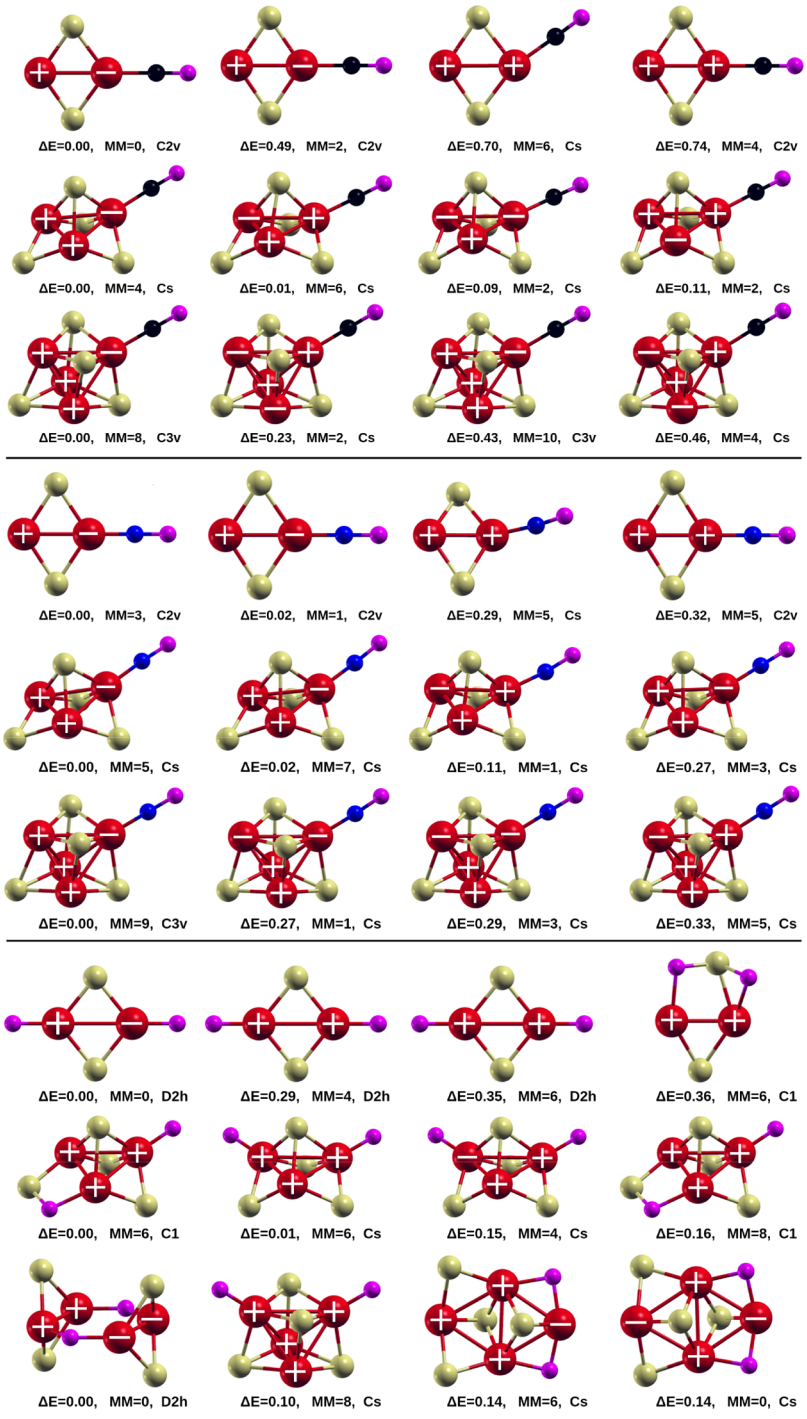

Figure 2. Putative lowest-energy structures of freestanding Fe_2S_2, Fe_3S_4, and Fe_4S_4 clusters upon adsorption of CO (first panel), NO (second panel), and O_2 (third panel), with their relative total energy ΔE (eV), their corresponding point-group symmetry, and total magnetic moment MM (in units of μ_B). The sign of the spin polarization of the iron atoms is indicated by + and − inside the atomic spheres in order to illustrate the magnetic couplings. Fe (red), S (yellow), O (magenta), C (black), and N (blue) spheres represent the different atoms of the clusters.

The ground-state geometry of Fe_3S_4 is also consistent with the structure observed in proteins.[55−58] It has C_{3v} symmetry and is formed by an Fe trimer capped by the S atoms (Figure 1). Its total spin moment of 4 μ_B comes from antiparallel couplings: one Fe atom (−2.93 μ_B) has opposite spin to the others (3.18 μ_B), and the sulfur atoms are weakly polarized (0.43, 0.14, 2 × 0.00 μ_B). A spin excitation of ferromagnetic kind with high spin (10 μ_B) lies at 0.06 eV above the ground state. The spin state where two Fe atoms have opposite magnetic moments and the third one remains unpolarized is noticeably less stable (ΔE = 0.36 eV) because of the magnetic frustration of one of the Fe atoms. Despite this fact, the noncollinear magnetic order does not arise. We note that the geometrical structure of the anionic state is similar to that of the neutral one, with slight relaxations, but with a total moment of 11 μ_B which differs by 1 μ_B with respect to that of the first neutral isomer (10 μ_B) and by 7 μ_B with respect to that of the neutral ground state (4 μ_B). This means a strong

DOI: 10.1021/acs.jpca.9b08201
J. Phys. Chem. A 2019, 123, 10919−10929

relaxation of the electronic density upon the electron excess despite the slight reconstruction of the atomic skeleton.

The lowest-energy structure of Fe_4S_4 is a tetrahedron Fe skeleton capped by sulfur atoms (C_{3v} symmetry). One can identify Fe and S atoms located at alternate vertices where each face is a planar rhombic Fe_2S_2 (Figure 1), thus reflecting the high stability of such unit. Because of its C_{3v} symmetry, it has three equivalent Fe−Fe bonds of 2.38 Å and three bonds of 2.61 Å. Here also the cluster exhibits a similarity with the structure in proteins. The most stable spin state is of antiparallel type where one Fe atom (−2.52 μ_B) has opposite spin to the three others (3.26 μ_B). The sulfur atom linking the three equivalent iron atoms is substantially polarized (0.35 μ_B), whereas the other three are less (3×0.13 μ_B). In our previous work,[18] using SIESTA,[40,41] we found a similar atomic structure with a different antiparallel spin arrangement (singlet state). This singlet state results at 0.18 eV from the ground state in the VASP calculation. It is important to note that if the majority of DFT calculations agree on the lowest-energy structures of Fe_2S_2, Fe_3S_4, and Fe_4S_4 clusters, they sometimes differ on their spin states. Of course, going beyond the DFT which relies on the electron density rather than on the wave functions would provide a better description of the electronic states. In particular, the low-energy states possess area-law entanglement,[59] reflecting the locality present in all physical systems regardless of interaction strength. In this context, a better approach was proposed by Sharma et al.,[13] which consists in solving numerically the valence many-particle quantum mechanical equations for iron−sulfur clusters. This kind of approaches implies, however, a more computational cost than DFT.

Interaction of Fe_2S_2, Fe_3S_4, and Fe_4S_4 Clusters with CO and NO: Molecular Adsorption. Figure 1 also depicts the most stable atomic arrangements of Fe_2S_2, Fe_3S_4, and Fe_4S_4 after CO adsorption, with their point-group symmetry and their spin states. The most stable atomic configurations are those with CO adsorbed molecularly instead of dissociatively. The resulting C−O bond length is less than 2% larger than that of the unadsorbed molecule, and the atomic structure of the host Fe−S cluster is preserved to a large extent. CO binds to a single Fe atom through C; it does not bind to S neither via O nor via C, and the binding to Fe through O leads to a very excited isomer. The main effect of the CO attack from the structural point of view is an enlargement of the Fe−Fe interatomic distances (about 10%) and a shrinking of the Fe−S ones (about 7% in some cases).

From the electronic point of view, the main effect of the CO attack is to reduce the spin polarization of the cluster and to modify the magnetic couplings. The reduction of the spin polarization is reflected in the lower local magnetic moments of the host cluster atoms, particularly of the Fe atom in contact with C. With regard to the magnetic couplings, the Fe atom binds to CO couples antiparallel to the rest of Fe atoms and to the C atom of the molecule (whose magnetic moment does not exceed 0.02 μ_B). Although a clear spin-polarized charge density redistribution takes place upon CO adsorption in all clusters, for Fe_3S_4 and Fe_4S_4 this is not reflected in their total magnetic moment which remains unchanged with respect to the pristine clusters. On the contrary, the effect is dramatic in the case of Fe_2S_2 whose total moment completely quenches upon CO adsorption. Therefore, adsorption of this light molecule establishes a mechanism to access the antiferromagnetic-like spin isomer of the host with 0 μ_B. An antiparallel magnetic order with a total moment of 2 μ_B (Figure 2) is the next low-lying isomer in this structure but with a large energy difference of 0.49 eV.

The most stable atomic arrangements of Fe_2S_2, Fe_3S_4, and Fe_4S_4 after NO adsorption are also reported in Figure 1, with their point-group symmetry and their spin states. The attack of the Fe−S clusters by NO leads to the same scenario as that found with CO and discussed in the previous paragraphs. The only slight differences are that (i) the local spin polarization of the Fe atom in contact with N is reduced to a larger extent now than upon adsorption of CO, while the opposite happens to the rest of Fe atoms; (ii) the local magnetic moment of the N atom (between 0.18 and 0.25 μ_B) is larger than that found on the C atom; (iii) because of the marked imbalance in the local moments on the Fe atoms, the total moment of Fe_2S_2−NO is noticeably reduced but not completely quenched like in Fe_2S_2−CO; (iv) because of the odd number of valence electrons when NO is adsorbed instead of CO, the total moments are odd and increase by 1 μ_B in Fe_3S_4−NO and Fe_4S_4−NO instead of remaining unaffected.

Interaction of Fe_2S_2, Fe_3S_4, and Fe_4S_4 Clusters with O_2: Dissociative Adsorption. In contrast to the molecular adsorption of CO and NO on the Fe−S host clusters, the most stable configurations upon O_2 attack are those where the molecule is dissociated and the two oxygen atoms bind separately to Fe atoms. This trend is consistent with the fact that among the three light molecules considered, O_2 has the lowest dissociation energy because it has two more antibonding molecular orbitals occupied than CO and one more than NO. The dissociative chemisorption leads to significant structural distortions of the host cluster. Moreover, the high electronegativity of the oxygen atoms as compared to that of Fe strongly affects the spin-polarized electronic charge redistribution and the exchange coupling between the iron sites, which leads to changes in the magnetic couplings. In general, oxygen tends to reduce the spin polarization in Fe (smaller local moments than upon CO and NO attack) and to weaken the Fe−Fe interaction inducing antiparallel couplings that in some cases (Fe_4S_4) clearly arise from indirect Fe−Fe exchange coupling mediated by O.

Fe_2S_2 with O_2. The structure of the ground state (D_{2h} symmetry) is an atomic arrangement where the oxygen atoms bind separately the two Fe atoms of a planar rhombic Fe_2S_2 cluster (Figure 1). The magnetic state corresponds to a singlet resulting from an antiparallel Fe−Fe coupling (±2.43 μ_B) and parallel Fe−O coupling (2.43/0.36 μ_B), while the sulfur atoms remain unpolarized. The chemisorption gives rise to a noticeable enlargement (20%) of the Fe−Fe interatomic distance and slightly shortened (5%) Fe−S bonds with respect to the isolated Fe_2S_2 cluster (Figure 1). A ferromagnetic-like order with a total moment of 4 μ_B in this cluster is the first spin isomer (Figure 2), well above the ground state from the energetic point of view (0.29 eV). In this spin isomer, the Fe−Fe bond is also enlarged (19%). In the most stable molecular adsorption of O_2, the molecule anchors to an Fe atom. This isomer lies at 2.36 eV above the ground state, a huge amount of energy. The results indicate that a multiple barrier process exists in the energy landscape to pass from the molecular adsorption to the dissociative ground state because not only the barrier for dissociation has to be overcome but also a diffusion barrier for the two oxygen atoms to finally locate at opposite sides of the cluster, each one anchored to an Fe atom. This also holds for the other Fe−S clusters studied in this work

DOI: 10.1021/acs.jpca.9b08201
J. Phys. Chem. A 2019, 123, 10919−10929

and demonstrates that the kinetics of the oxidation process of these nanoparticles is relatively complex. Calculation of barriers for such reactions is not the scope of the present work, but previous authors have addressed this problem.[30]

Another interesting result of the Fe_2S_2−O_2 interaction is the electronic and magnetic structure of the corresponding anionic state. Except small relaxations, its geometrical structure is similar to that of its neutral counterpart, but it has a total spin moment of 5 μ_B, while the neutral ground state has 0 μ_B (singlet state). It is surprising that an electron excess changes the moment in much more than just 1 μ_B if the geometry remains practically unchanged. This clearly points again to a quasi-purely electronic effect. In order to analyze the origin of such behavior in this system, we plot in Figure 3 both the

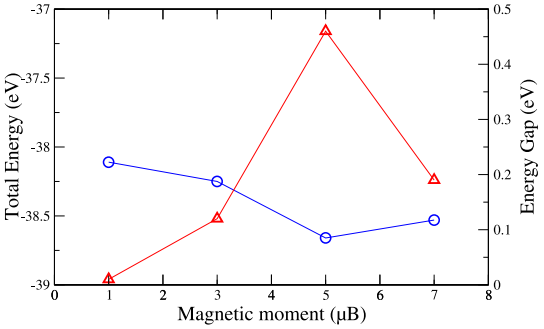

Figure 3. Total energy (○) and HOMO−LUMO gap (△) for different spin isomers of the Fe_2S_2−O_2 anionic cluster with similar atomic skeleton (apart from slight distortions) as its corresponding neutral counterpart (Figure 1).

energy and the highest occupied molecular orbital (HOMO)−lowest unoccupied molecular orbital (LUMO) gap as a function of the total moment of the possible spin isomers of the anionic Fe_2S_2−O_2 cluster. The ground state corresponds to 5 μ_B than to 1 μ_B which is also less stable than 3 and 7 μ_B. It is interesting to note that a perfect correlation exists between the stability and the HOMO−LUMO gap, which in this case reaches a marked maximum exactly for the ground-state spin isomer of 5 μ_B. Because large gaps are usually good indicators of cluster stability, it is clear that a strong electronic relaxation is energetically favorable upon an electron capture, leading to a ferromagnetic-like order with a total moment of 5 μ_B. The densities of electronic states around the Fermi energy, shown in Figure 4, provide a deeper insight on the energy spectrum associated with the different spin-polarized electronic densities for the states with 1 and 5 μ_B and in particular on the opening of the large HOMO−LUMO gap upon the electron capture in Fe_2S_2−O_2.

Fe_3S_4 with O_2. In this case, two geometrical structures of C_1 and C_s symmetries but with the same total magnetic moment of 6 μ_B differ by only 6 meV of energy (Figure 2). By including the zero-point energy correction obtained from the vibrational analysis, the energy difference increases to 10 meV in favor of the structure of the C_1 symmetry (see Figure 1 for more details). It consists of the Fe_3S_4 host cluster where one oxygen binds one iron atom and the other breaks one of the Fe−S bonds to create an −Fe−O−S− bridge. Its total moment results from a low-spin ferromagnetic-like state. The most coordinated Fe atom (6 bonds) bears the lowest moment (0.8 μ_B). A symmetric structure where both oxygen atoms form −Fe−O−S− bridges in the host Fe_3S_4 cluster is largely

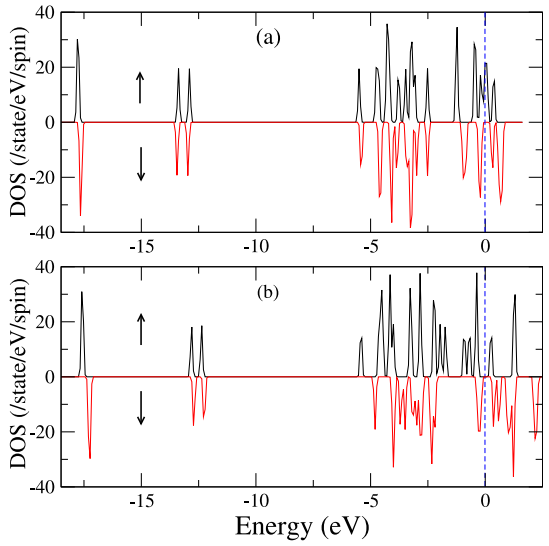

Figure 4. : Calculated spin-polarized (↑, ↓) densities of states for the anionic Fe_2S_2−O_2 cluster with total moments of 1 (a) and 5 μ_B (b). The vertical dashed line indicates the Fermi level.

unstable with ΔE = 0.42 eV (figure not shown). Binding separately the two oxygen atoms to two distinct iron atoms (C_s symmetry) leads to the first isomer with the same total moment of 6 μ_B (Figure 2). The interatomic distance between Fe atoms anchored with oxygen is the most enlarged one (22%). The effect of O_2 attack to Fe_3S_4 is thus very subtle. Unexpectedly, it increases the total magnetic moment from 4 μ_B of the isolated Fe_3S_4 cluster to 6 μ_B of Fe_3S_4−O_2, but a deep analysis demonstrates that on the one hand oxidation reduces noticeably the spin polarization, but on the other hand the magnetic configuration changes from antiparallel to parallel. The overall balance results in a larger total moment that arises from a low-spin ferromagnetic-like state.

Fe_4S_4 with O_2. The adsorption of O_2 on Fe_4S_4 has a dramatic effect. In this case, the structure of Fe_4S_4 is broken into two Fe_2S_2 entities linked through the two oxygen atoms via −Fe−O−Fe− bonds of 1.75 Å (Figure 1). This ground-state structure of D_{2h} symmetry is antiferromagnetically ordered (zero total moment) with opposite iron spin moments of the Fe_2S_2 substructures (±3.02 μ_B) whose exchange coupling is indirect (mediated by O). The sulfur atoms bear moments of ±0.32 μ_B parallel to those of iron, whereas the oxygen atoms remain unpolarized. Therefore, the adsorption of O_2 completely quenches the magnetic moment of the system. The Fe−Fe bond in each Fe_2S_2 unit is enlarged by only 10%, and the Fe−S bond is almost unchanged (+2%) with respect to the isolated Fe_2S_2 cluster (Figure 1). This means that the Fe_2S_2 subcluster preserves its identity (structural and magnetic) to a large extent. We remark that the Fe_2S_2 entities form the structural basis not only of Fe_3S_4 and Fe_4S_4 (which are the ones most frequently contained in proteins) but also of larger Fe−S clusters contained or not in proteins. They are involved in a number of fundamental processes required for life,[60] and one could also speculate on their fundamental role in protein synthesis.

Binding separately the two oxygen atoms to two active iron sites of the original Fe_4S_4 cluster leads to the first isomer with relative total energy ΔE = 0.10 eV (Figure 2). It has C_s symmetry and a total moment of 8 μ_B, exactly the same as the isolated Fe_4S_4 cluster, but resulting from a ferromagnetic-like

DOI: 10.1021/acs.jpca.9b08201
J. Phys. Chem. A 2019, 123, 10919−10929

order in the Fe subcluster in which, due to the Fe−O interaction, the spin polarization of the O-bonded Fe atoms tends to vanish (0.57 μ_B), while it is approximately 6 times larger (3.00 μ_B) on the two other Fe sites. The induced moments on the nonequivalent S atoms are 0.04 and 0.18 μ_B, whereas the oxygen atoms bear 0.22 μ_B. The interaction of Fe with the electronegative oxygen atom enlarges the corresponding Fe−Fe bonds by 19% and leads to parallel iron spins instead of the antiparallel coupling found in the isolated Fe_4S_4 cluster (Figure 1). Again, the isomer with O_2 molecularly adsorbed on an iron atom of the pristine structure is a very excited metastable state, with ΔE = 1.66 eV (figure not shown).

An interesting result in this system is that, as in Fe_2S_2−O_2, an electron excess induces important changes, although in this case it is the atomic skeleton that is strongly affected. The ground-state atomic structure of the anionic state of Fe_4S_4−O_2 does not correspond to that of its neutral counterpart, even not to its first structural isomer but to the second one (Figure 2). We report in Figure 5 the four first putative lowest-energy

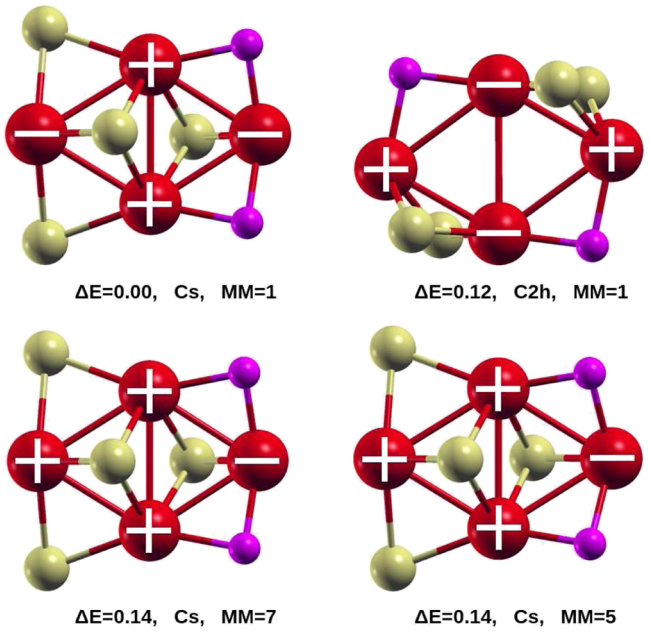

Figure 5. Putative lowest-energy structures of the fourth first isomers of the $Fe_4S_4^-$ anionic cluster upon O_2 adsorption, with their corresponding relative total energy ΔE (eV), point-group symmetry, and total magnetic moment MM (in units of μ_B). The sign of the spin polarization of the iron atoms is indicated by + and − inside the atomic spheres in order to illustrate the magnetic couplings. Red, yellow, and magenta spheres represent Fe, S, and O atoms, respectively.

structures of the anionic Fe_4S_4−O_2 clusters. Despite the noticeable structural change upon electron capture, the magnetic moment change is just 1 μ_B. However, it is also remarkable that the same atomic configuration in the neutral state (second isomer of the neutral system) has 6 μ_B.

Absolute Stability and Electronic Indicators. The binding energies (BEs) per atom for Fe_2S_2, Fe_3S_4, and Fe_4S_4 host clusters and the resulting systems upon CO, NO, and O_2 adsorption are plotted in Figure 6. The BE is calculated from the following expression, where X = C, N, O

$$\mathrm{BE}(\mathrm{Fe}_n\mathrm{S}_m) - \mathrm{XO} = [nE(\mathrm{Fe}) + mE(\mathrm{S}) + E(\mathrm{X}) + E(\mathrm{O}) - E(\mathrm{Fe}_n\mathrm{S}_m - \mathrm{XO})]/(n + m + 2)$$

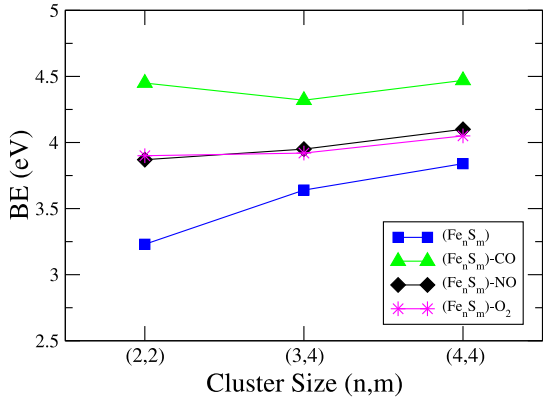

Figure 6. Calculated BE per atom of Fe_2S_2, Fe_3S_4, and Fe_4S_4 and the corresponding clusters upon CO, NO, and O_2 adsorption.

The results obtained demonstrate that the three molecules enhance the stability of the multicenter Fe_2S_2, Fe_3S_4, and Fe_4S_4 clusters but more substantially with CO than with NO and O_2, which contribute with almost the same amount. Besides, this increase is more important for Fe_2S_2 than for the two other host clusters and reaches 38% with CO. This result can explain the experimental findings of Yin et al.[6] who showed that the reaction of Fe_mS_m (m = 1−4) clusters with CO is observed only for m = 1 to form carbonyl sulfide FeS−CO and for m = 2 to give rise to the formation of the Fe_2S_2CO product. Neither reaction nor associated products are observed with Fe_3S_3 and Fe_4S_4 species.

The calculated VDE and the AEA of the studied clusters are reported in Figure 7. We also include the data available for Fe_2S_2, Fe_3S_3, and Fe_4S_4 in the literature from two experimental

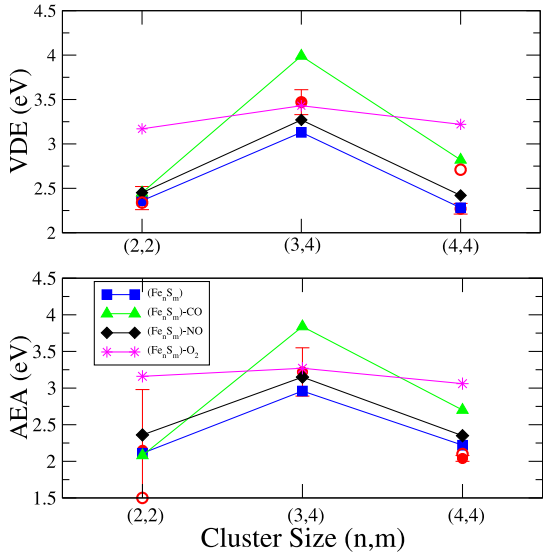

Figure 7. Calculated VDE and AEA of Fe_2S_2, Fe_3S_4, and Fe_4S_4 and the corresponding clusters upon CO, NO, and O_2 adsorption. The available experimental values of VDE and AEA (red •)[5] and (red ○)[7] for Fe_2S_2, Fe_3S_4, and Fe_4S_4 clusters are also included for the sake of comparison.

DOI: 10.1021/acs.jpca.9b08201
J. Phys. Chem. A 2019, 123, 10919−10929

groups.[5,7] We note that these experimental data present discrepancies, important in some cases. The VDE of the clusters is calculated as the energy difference between that of the anionic cluster and that of the neutral counterpart with the structure of the anionic cluster. It corresponds to the ionization energy of the anion species. Except the calculated values of VDE of Fe_3S_4 (3.13 eV) which is within 0.2 eV of the lowest experimental value (3.47 ± 0.14 eV) and AEA of Fe_4S_4 (2.22 eV) which exceeds the highest experimental value (2.04 ± 0.04 eV) by 0.14 eV, the theoretical data fall within the range of the measured values of Nakajima et al.[5] With respect to the experimental data of Yin and Bernstein,[7] our calculated VDE value for Fe_2S_2 (2.36 eV) is in good agreement with the experimental one (2.34 eV), while for Fe_4S_4, it is lower (2.28 eV) than the measured value (2.71 eV). The calculated AEAs for Fe_2S_2 (2.11 eV) and for Fe_4S_4 (2.22 eV) are slightly higher than their respective experimental values 1.5 and 2.10 eV. The agreement between our theoretical and the experimental data can then be considered as fairly good and comparable to the more recent theoretical results.[7] This gives further support to our ground-state configurations. The molecular adsorption of CO increases the VDE of Fe_3S_4 and Fe_4S_4 clusters by ∼27% and leaves unchanged that of Fe_2S_2. The effect of NO on the VDE of the three clusters is weak (3, 4, and 5%, respectively). The most noticeable change is produced by the interaction with O_2 upon the dissociative adsorption described in the previous section. The chemisorption of O_2 substantially increases the values of the VDE by 34, 10, and 46% for Fe_2S_2, Fe_3S_4, and Fe_4S_4, respectively. As discussed in the previous section, the chemisorption of O_2 on Fe_3S_4 and Fe_4S_4 breaks an Fe−S bond in Fe_3S_4 and separates the Fe_4S_4 structure into two Fe_2S_2 units, while Fe_2S_2 undergoes relatively important Fe−Fe bond elongation (20%) (Figure 1). Except the relatively important effect of NO on the AEA of Fe_2S_2 as compared to the corresponding VDE change, one can note similar qualitative effects of CO, NO, and O_2 on the AEAs of the host clusters (Figure 7).

CONCLUSIONS

The structural and electronic properties of Fe_2S_2, Fe_3S_4, and Fe_4S_4 clusters attacked by NO, CO, and O_2 oxidants were investigated in the framework of DFT within the generalized gradient approximation to exchange and correlation. CO and NO bind molecularly to these iron sulfide clusters. They bind through an Fe atom via C or N, leading to moderate relaxations in the host clusters that essentially consist in an enlargement of the Fe−Fe interatomic distances and a shrinking of the Fe−S ones. In contrast, the most stable configurations upon O_2 attack are those where the molecule is dissociated and the two oxygen atoms bind separately to Fe atoms. This chemisorption leads to significant structural distortions in Fe_2S_2 and Fe_3S_4 and to the breaking of the Fe_4S_4 skeleton into two Fe_2S_2 subclusters linked via oxygen. Molecular adsorption of O_2 is a quite excited metastable state, and both molecular to dissociative and diffusion barriers have to be overcome to connect this with the ground state.

The three molecules, but particularly CO, enhance the stability of the iron−sulfur clusters. This increase is noticeably more pronounced for Fe_2S_2 than for the other clusters, a result that correlates with the fact that in recent experiments of Fe_mS_m (m = 1−4) reaction with CO, Fe_2S_2CO results as a prominent product.

From the electronic point of view, the main effect of the CO and NO attack is to reduce the spin polarization of the cluster and to modify the magnetic couplings. The reduction of the spin polarization is reflected in the lower local magnetic moments of the host cluster atoms, particularly of the Fe atom in contact with C or N. With regard to the magnetic couplings, the Fe atom is linked to CO or NO couples antiparallel to the rest of Fe atoms as well as to the C or N atom of the molecule. The effect is dramatic in the case of Fe_2S_2 whose total moment (8 μ_B) completely quenches upon CO adsorption. Therefore, adsorption of CO establishes a mechanism to access the antiferromagnetic-like spin isomer of the host in the singlet state. The effect of O_2 chemisorption on the spin-polarized electronic structure is quite noticeable and somehow expected in view of the strong induced structural distortions. Oxygen tends to strongly reduce the spin polarization in Fe and to weaken the Fe−Fe interaction inducing antiparallel couplings that in the case of Fe_4S_4 clearly arise from indirect Fe−Fe exchange coupling mediated by O, leading to a completely quenched total magnetic moment.

Finally, the VDE and the EA increase upon reaction with all these light molecules but in particular with O_2.

AUTHOR INFORMATION

Corresponding Author

*E-mail: famitouche@yahoo.fr.

ORCID

Fadila Amitouche: 0000-0002-5505-7659

Said Bouarab: 0000-0002-2762-3123

Notes

The authors declare no competing financial interest.

ACKNOWLEDGMENTS

We acknowledge the financial support from the Algerian Ministry of Higher Education and Scientific Research via the project PRFU B00L02UN150120180005, from the Junta de Castilla y León in Spain (project no. VA124G18), and from the Spanish Ministry of Economy and Competitiveness (project PGC2018-093745-B-100). The last research project is partially supported by FEDER.

REFERENCES

(1) Beinert, H. Iron-Sulfur Proteins: Ancient Structures, Still Full of Surprises. *J. Biol. Inorg Chem.* **2000**, *5*, 2−15.

(2) Beinert, H.; Holm, R. H.; Münck, E. Iron-Sulfur Clusters: Nature's Modular, Multipurpose Structures. *Science* **1997**, *277*, 653−659.

(3) Bill, E. Iron-sulfur clusters-new features in enzymes and synthetic models. *Hyperfine Interact.* **2012**, *205*, 139−147.

(4) Zhang, N.; Hayase, T.; Kawamata, H.; Nakao, K.; Nakajima, A.; Kaya, K. Photoelectron Spectroscopy of Iron-Sulfur Cluster Anions. *J. Chem. Phys.* **1996**, *104*, 3413−3419.

(5) Nakajima, A.; Hayase, T.; Hayakawa, F.; Kaya, K. Study on iron-sulfur cluster in gas phase: electronic structure and reactivity. *Chem. Phys. Lett.* **1997**, *280*, 381−389.

(6) Yin, S.; Wang, Z.; Bernstein, E. R. Formaldehyde and methanol formation from reaction of carbon monoxide and hydrogen on neutral Fe2S2 clusters in the gas phase. *Phys. Chem. Chem. Phys.* **2013**, *15*, 4699−4706.

(7) Yin, S.; Bernstein, E. R. Photoelectron Spectroscopy and Density Functional Theory Studies of Iron Sulfur $(FeS)_m^-$ (m=2-8) Cluster Anions: Co-existing Multiple Spin States. *J. Chem. Phys.* **2017**, *121*, 7362.

DOI: 10.1021/acs.jpca.9b08201
J. Phys. Chem. A 2019, 123, 10919−10929

(8) Sigfridsson, E.; Olsson, M. H. M.; Ryde, U. Inner-Sphere Reorganization Energy of Iron−Sulfur Clusters Studied with Theoretical Methods. *Inorg. Chem.* **2001**, *40*, 2509−2519.
(9) Torres, R. A.; Lovell, T.; Noodleman, L.; Case, D. A. Density Functional and Reduction Potential Calculations of Fe4S4Clusters. *J. Am. Chem. Soc.* **2003**, *125*, 1923−1936.
(10) Dey, A.; Glaser, T.; Moura, J. J.-G.; Holm, R. H.; Hedman, B.; Hodgson, K. O.; Solomon, E. I. Ligand K-edge X-ray Absorption Spectroscopy and DFT Calculations on [Fe3S4]0,+Clusters: Delocalization, Redox, and Effect of the Protein Environment. *J. Am. Chem. Soc.* **2004**, *126*, 16868−16878.
(11) Jensen, K. P. Computational studies of modified [Fe3S4] clusters: Why iron is optimal. *J. Inorg. Biochem.* **2008**, *102*, 87−100.
(12) Bhave, D. P.; Han, W.-G.; Pazicni, S.; Penner-Hahn, J. E.; Carroll, K. S.; Noodleman, L. Geometric and Electrostatic Study of the [4Fe-4S] Cluster of Adenosine-5′-Phosphosulfate Reductase from Broken Symmetry Density Functional Calculations and Extended X-ray Absorption Fine Structure Spectroscopy. *Inorg. Chem.* **2011**, *50*, 6610−6625.
(13) Sharma, S.; Sivalingam, K.; Neese, F.; Chan, G. K.-L. Low-energy Spectrum of Iron-Sulfur Clusters Directly from Many-Particle Quantum Mechanics. *Nat. Chem.* **2014**, *6*, 927−933.
(14) Shoji, M.; Koizumi, K.; Taniguchi, T.; Kitagawa, Y.; Yamanaka, S.; Okumura, M.; Yamaguchi, K. Theory of Chemical Bonds in Metalloenzymes III: Full Geometry Optimization and Vibration Analysis of Ferredoxin-type [2Fe-2S] Cluster. *Int. J. Quantum Chem.* **2007**, *107*, 116−133.
(15) Bergeler, M.; Stiebritz, M. T.; Reiher, M. Structure-Property Relationships of Fe4S4Clusters. *ChemPlusChem* **2013**, *78*, 1082−1098.
(16) Hübner, O.; Sauer, J. The Electronic States of $Fe_2S_2^{-/0/+/2+}$. *J. Chem. Phys.* **2002**, *116*, 617−628.
(17) Hübner, O.; Sauer, J. Structure and Thermochemistry of $Fe_2S_2^{/0/+}$ Gas Phase Clusters and their Fragments. B3LYP Calculations. *Phys. Chem. Chem. Phys.* **2002**, *4*, 5234−5243.
(18) Tazibt, S.; Bouarab, S.; Ziane, A.; Parlebas, J. C.; Demangeat, C. Electronic, Magnetic and Structural Properties of Neutral, Cationic and Anionic Fe_2S_2, Fe_3S_4 and Fe_4S_4 Clusters. *J. Phys. B: At., Mol. Opt. Phys.* **2010**, *43*, 165101.
(19) Ding, L.-P.; Kuang, X.-Y.; Shao, P.; Zhong, M.-M. Probing the Structural, Electronic and Magnetic Properties of Multicenter $Fe_2S_2^{0/-}$, $Fe_3S_4^{0/-}$and $CFe_4S_4^{0/-}$lusters. *J. Mol. Model.* **2013**, *19*, 1527−1536.
(20) Uzunova, E. L.; Mikosch, H. Electronic, Magnetic Structure and Water Splitting Reactivity of the Iron-Sulfur Dimers and their Hexacarbonyl Complexes: A Density Functional Study. *J. Chem. Phys.* **2014**, *141*, 044307−044314.
(21) Kennedy, M. C.; Antholine, W. E.; Beinert, H. An EPR Investigation of the Products of the Reaction of Cytosolic and Mitochondrial Aconitases with Nitric Oxide. *J. Biol. Chem.* **1997**, *272*, 20340−20347.
(22) Gardner, P. R.; Costantino, G.; Szabó, C.; Salzman, A. L. Nitric Oxide Sensitivity of the Aconitases. *J. Biol. Chem.* **1997**, *272*, 25071−25076.
(23) Furukawa, T.; Kohno, H.; Tokunaga, R.; Taketani, S. Nitric Oxide-Mediated Inactivation of Mammalian Ferrochelatase in Vivo and in Vitro: Possible Involvement of the Iron-Sulphur Cluster of the Enzyme. *Biochem. J.* **1995**, *310*, 533−538.
(24) Sellers, V. M.; Johnson, M. K.; Dailey, H. A. Function of the [2Fe−2S] Cluster in Mammalian Ferrochelatase: A Possible Role as a Nitric Oxide Sensor†. *Biochemistry* **1996**, *35*, 2699−2704.
(25) Cooper, C. E. Nitric Oxide and Iron Proteins. *Biochim. Biophys. Acta* **1999**, *1411*, 290−309.
(26) Rouault, T.; Klausner, R. D. Iron-sulfur clusters as biosensors of oxidants and iron. *Trends Biochem. Sci.* **1996**, *21*, 174−177.
(27) Outten, F. W. Iron-Sulfur Clusters as Oxygen-Responsive Molecular Switches. *Nat. Chem. Biol.* **2007**, *3*, 206−207.
(28) Crack, J. C.; Green, J.; Thomson, A. J.; Le Brun, N. E. Iron-Sulfur Cluster Sensor-Regulators. *Curr. Opin. Chem. Biol.* **2012**, *16*, 35−44.
(29) Crack, J. C.; Green, J.; Hutchings, M. I.; Thomson, A. J.; Le Brun, N. E. Bacterial Iron-Sulfur Regulatory Proteins as Biological Sensor-Switches. *Antioxid. Redox Signaling* **2012**, *17*, 1215−1231.
(30) Finkelmann, A. R.; Stiebritz, M. T.; Reiher, M. Activation Barriers of Oxygen Transformation at the Active Site of [FeFe] Hydrogenases. *Inorg. Chem.* **2014**, *53*, 11890−11902.
(31) Bruska, M. K.; Stiebritz, M. T.; Reiher, M. Analysis of Differences in Oxygen Sensitivity of Fe-S Clusters. *Dalton Trans.* **2013**, *42*, 8729−8735.
(32) Bruska, M. K.; Stiebritz, M. T.; Reiher, M. Regioselectivity of H Cluster Oxidation. *J. Am. Chem. Soc.* **2011**, *133*, 20588−20603.
(33) Holm, R. H.; Ciurli, S.; Weigel, J. A. *Subsite-Specific Structures and Reactions in Native and Synthetic [4Fe-4S] Cubane-Type Clusters*. Progress in Inorganic Chemistry; Wiley, 2007; Vol. *38*, pp 1−74.
(34) Crack, J. C.; Gaskell, A. A.; Green, J.; Cheesman, M. R.; Le Brun, N. E.; Thomson, A. J. Influence of the Environment on the [4Fe−4S]2+to [2Fe−2S]2+Cluster Switch in the Transcriptional Regulator FNR. *J. Am. Chem. Soc.* **2008**, *130*, 1749−1758.
(35) Jervis, A. J.; Crack, J. C.; White, G.; Artymiuk, P. J.; Cheesman, M. R.; Thomson, A. J.; Le Brun, N. E.; Green, J. The O2 sensitivity of the transcription factor FNR is controlled by Ser24 modulating the kinetics of [4Fe-4S] to [2Fe-2S] conversion. *Proc. Natl. Acad. Sci. U.S.A.* **2009**, *106*, 4659−4664.
(36) Kresse, G.; Hafner, J. Ab initiomolecular dynamics for liquid metals. *Phys. Rev. B: Condens. Matter Mater. Phys.* **1993**, *47*, 558−561.
(37) Blöchl, P. E. Projector Augmented-Wave Method. *Phys. Rev. B: Condens. Matter Mater. Phys.* **1994**, *50*, 17953−17979.
(38) Kresse, G.; Joubert, D. From ultrasoft pseudopotentials to the projector augmented-wave method. *Phys. Rev. B: Condens. Matter Mater. Phys.* **1999**, *59*, 1758−1775.
(39) Perdew, J. P.; Burke, K.; Ernzerhof, M. Generalized Gradient Approximation Made Simple. *Phys. Rev. Lett.* **1996**, *77*, 3865−3868.
(40) Soler, J. M.; Artacho, E.; Gale, J. D.; García, A.; Junquera, J.; Ordejón, P.; Sánchez-Portal, D. The SIESTA method forab initioorder-Nmaterials simulation. *J. Phys.: Condens. Matter* **2002**, *14*, 2745−2779.
(41) Ordejón, P.; Artacho, E.; Soler, J. M. Self-consistent order-Ndensity-functional calculations for very large systems. *Phys. Rev. B: Condens. Matter Mater. Phys.* **1996**, *53*, R10441−R10444.
(42) Henkelman, G.; Arnaldsson, A.; Jónsson, H. A Fast and Robust Algorithm for Bader Decomposition of Charge Density. *Comput. Mater. Sci.* **2006**, *36*, 354−360.
(43) Sanville, E.; Kenny, S. D.; Smith, R.; Henkelman, G. Improved Grid-Based Algorithm for Bader Charge Allocation. *J. Comput. Chem.* **2007**, *28*, 899−908.
(44) Tang, W.; Sanville, E.; Henkelman, G. A grid-Based Bader Analysis Algorithm without Lattice Bias. *J. Phys.: Condens. Matter* **2009**, *21*, 084204.
(45) Tazibt, S.; Chikhaoui, A.; Bouarab, S.; Vega, A. Structural, Electronic, and Magnetic Properties of Iron Disulfide $Fe_nS_2^{0\pm}$(n=1-6) Clusters. *J. Phys. Chem. A* **2017**, *121*, 3768−3780.
(46) Huber, K. P.; Herzberg, G. *Molecular Spectra and Molecular Structure. IV. Constants of Diatomic Molecules*; Springer, 1979.
(47) Reiher, M.; Salomon, O.; Artur Hess, B. Reparameterization of Hybrid Functionals Based on Energy Differences of States of Different Multiplicity. *Theor. Chem. Acc. Theory Comput. Model.* **2001**, *107*, 48−55.
(48) Paulsen, H.; Duelund, L.; Winkler, H.; Toftlund, H.; Trautwein, A. X. Free Energy of Spin-Crossover Complexes Calculated with Density Functional Methods. *Inorg. Chem.* **2001**, *40*, 2201−2203.
(49) Barrow, R. F.; Cousins, C. Spectroscopic Properties of the Gaseous Diatomic Sulfides. *Adv. High Temp. Chem.* **1971**, *4*, 161−170.
(50) DeVore, T. C.; Franzen, H. F. First Period Transition Metal Sulfide Gaseous Molecule: Matrix Spectra, Oxide−Sulfur Correlation,

DOI: 10.1021/acs.jpca.9b08201
J. Phys. Chem. A 2019, 123, 10919−10929

and Trends [500 to 600 cm/sup-1/]. *High Temp. Sci.* **1975**, *7*, 220−235, DOI: 10.2172/5099999.
(51) Harvey, J. N.; Heinemann, C.; Fiedler, A.; Schröder, D.; Schwarz, H. Redox Properties of the Diatomic Bare Iron Chalcogenides FeO and FeS in the Gas Phase. *Chem.−Eur. J.* **1996**, *2*, 1230−1234.
(52) Zhai, H.-J.; Kiran, B.; Wang, L.-S. Electronic and Structural Evolution of Monoiron Sulfur Clusters, FeS_{n-} and FeS_n (n=1-6), from Anion Photoelectron Spectroscopy. *J. Phys. Chem. A* **2003**, *107*, 2821−2828.
(53) Kiley, P. J.; Beinert, H. The Role of Fe-S Proteins in Sensing and Regulation in Bacteria. *Curr. Opin. Microbiol.* **2003**, *6*, 181−185.
(54) Nakajima, A.; Kawamata, H.; Hayase, T.; Negishi, Y.; Kaya, K. Photoelectron Spectroscopy of Transition Metal-Sulfur Cluster Anions. *Z. Physik D Atoms, Mol. Clust.* **1997**, *40*, 17−21.
(55) Mayerle, J. J.; Denmark, S. E.; DePamphilis, B. V.; Ibers, J. A.; Holm, R. H. Synthetic analogs of the active sites of iron-sulfur proteins. XI. Synthesis and properties of complexes containing the iron sulfide (Fe2S2) core and the structures of bis[o-xylyl-.alpha.,.alpha.'-dithiolato-.mu.-sulfido-ferrate(III)] and bis[p-tolylthiolato-.mu.-sulfido-ferrate(III)] dianions. *J. Am. Chem. Soc.* **1975**, *97*, 1032−1045.
(56) Krebs, C.; Agar, J. N.; Smith, A. D.; Frazzon, J.; Dean, D. R.; Huynh, B. H.; Johnson, M. K. IscA, an Alternate Scaffold for Fe−S Cluster Biosynthesis†. *Biochemistry* **2001**, *40*, 14069−14080.
(57) Johnson, M. K.; Staples, C. R.; Duin, E. C.; Lafferty, M. E.; Duderstadt, R. E. Novel Roles for Fe-S Clusters in Stabilizing or Generating Radical Intermediates. *Pure Appl. Chem.* **1998**, *70*, 939−946.
(58) Rotsaert, F. A.; Pikus, J. D.; Fox, B. G.; Markley, J. L.; Sanders-Loehr, J. N-Isotope effects on the Raman spectra of Fe2S2 ferredoxin and Rieske ferredoxin: evidence for structural rigidity of metal sites. *J. Biol. Inorg Chem.* **2003**, *8*, 318−326.
(59) Hastings, M. B. Entropy and Entanglement in Quantum Ground States. *Phys. Rev. B: Condens. Matter Mater. Phys.* **2007**, *76*, 35114−35117.
(60) Mulder, D. W.; Boyd, E. S.; Sarma, R.; Lange, R. K.; Endrizzi, J. A.; Broderick, J. B.; Peters, J. W. Stepwise [FeFe]-hydrogenase H-cluster assembly revealed in the structure of HydAΔEFG. *Nature* **2010**, *465*, 248−251.

DOI: 10.1021/acs.jpca.9b08201
J. Phys. Chem. A 2019, 123, 10919−10929